1. Charinsak SAETIAW, 2. Jatuporn NAKORNTEP,
3. Vithaya CHAMNANPHRAI, 4. Suthasinee LAMULTREE

ORCID: 1. 0000-0002-0281-9947; 2. 0009-0001-9332-0462, 3. 0009-0003-7548-7108, 4. 0000-0003-3124-3980

DOI: 10.15199/48.2025.06.15

Design of a star-shaped patch antenna with a half-elliptical ground plane using copper thin film and PLA substrate

Projekt anteny łatowej w kształcie gwiazdy z półeliptyczną płytą uziemiającą, wykorzystującej cienką warstwę miedzi i podłoże PLA.

***Abstract**. This research focuses on the development and performance evaluation of a star-shaped patch antenna featuring a half-elliptical ground plane. Polylactic acid (PLA) is utilized as the substrate, while a thin copper film serves as the environmentally friendly conductive material. The objective is to explore cost-effective, reusable alternatives to conventional FR4 substrates, aiming to improve antenna efficiency and bandwidth through innovative geometric designs. The combination of the star-shaped patch and the modified ground plane is analyzed for its effects on critical parameters such as return loss, gain, and radiation patterns. The antenna operates across the entire ISM band (2.00 GHz to 3.08 GHz) with a center frequency of 2.45 GHz and achieves a gain of 2.32 dB. Prototype measurements revealed a - 10 dB impedance bandwidth ranging from 2.17 GHz to 3.11 GHz and a gain of 2.13 dB. Both simulation and experimental results confirm that the proposed design offers a sustainable, low-cost alternative to traditional FR4-based antennas.*

***Streszczenie.** Niniejsze badania koncentrują się na ocenie opracowania i wykonania projektu anteny łatowej w kształcie gwiazdy z pół-eliptyczną płytą uziemiającą. Jako podłoże zastosowano polilaktyd (kwas polimlekowy, ang. PLA) podczas gdy cienka warstwa miedzi stanowi przyjazny dla środowiska materiał przewodzący. Przedmiotem pracy jest zbadanie kosztowo oszczędnych, wielorazowych alternatyw dla tradycyjnych substratów FR4, w celu poprawy efektywności pracy anteny oraz szerokości pasma poprzez innowacyjne kształty geometryczne. Przeprowadzono analizę kombinacji łaty w kształcie gwiazdy oraz zmodyfikowanej płyty uziemiającej pod kątem wpływu na krytyczne parametry takiej jak strata odbiciowa, zysk energetyczny anteny i schematy promieniowania. Antena pracuje w całym pasmie ISM (2.00 GHz do 3.08 GHz) przy środkowej częstotliwości 2.45 GHz i osiąga zysk energetyczny 2.32 dB. Pomiary prototypu urządzenia wykazały szerokość pasma impedancji 10 dB w zakresie 2.17 GHz do 3.11 GHz oraz zysk 2.13 dB. Zarówno wyniki symulacji jak i doświadczalne potwierdzają że proponowana konstrukcja oferuje zrównoważoną, tanią pod względem kosztów alternatywę dla tradycyjnych anten opartych na FR4.*

Keywords: Star-shaped patch antenna; PLA substrate; ISM band; Modified ground plane
Słowa kluczowe: Antena łatowa w kształcie gwiazdy; podłoże PLA; pasmo ISM; zmodyfikowana płaszczyzna uziemiająca

1. Introduction

Wireless communication plays a vital role in modern technology by enabling seamless transmission of data and multimedia. Antennas are key components in these systems, where design parameters such as efficiency, bandwidth, and size are critical [1,2]. Microstrip patch antennas are widely favored due to their compact profile and ease of integration [3].

To enhance antenna performance, numerous design techniques have been investigated. Lamultree et al. [4] proposed a wideband circular monopole antenna for 5G applications, demonstrating significant improvements in bandwidth. Mondal and Sarkar [5] enhanced the gain and bandwidth of microstrip patch antennas using a modified ground plane, highlighting the importance of ground plane geometry. Similarly, Pandey and Chaudhary [6] developed a star-shaped microstrip patch antenna with defective structures to achieve broadband characteristics, illustrating the design potential of non-standard geometries for performance improvement.

Traditional fabrication methods using FR4 involve chemical etching, which generates hazardous waste [7]. Milling copper-clad laminates offers a more environmentally friendly alternative for prototyping, but the search for sustainable, biodegradable substrates remains ongoing. Jankowski-Mihułowicz et al. [8] emphasized the growing interest in recyclable or textile-based substrates for RFID and wearable applications.

Additive manufacturing offers a compelling alternative. Saetiaw and Phuchaduek [9] demonstrated that 3D-printed dipole antennas using conductive PLA filament could achieve functional wireless performance, highlighting the potential of low-cost materials. Aziz et al. [10] reviewed additive manufacturing techniques for antennas and concluded that 3D printing enables customized, efficient, and eco-friendly designs across frequency ranges.

To overcome the limitations of expensive conductive filaments and specialized printers, alternative methods using standard PLA substrates combined with low-cost copper thin films have been explored [11]. PLA is biodegradable, widely available, and compatible with standard FDM 3D printers, while copper foil provides excellent electrical conductivity at a significantly lower cost than conductive PLA. This hybrid approach offers a balance between environmental sustainability, material affordability, and reliable electrical performance.

Expanding on sustainable fabrication strategies, Helena et al. [12] evaluated three techniques for manufacturing 28 GHz horn antennas: metallizing PLA structures with copper tape, coating PLA with conductive spray paint, and direct 3D printing using conductive filament. Among these, the conductive filament method yielded the highest gain and widest bandwidth but required more expensive materials and specialized printing equipment. These findings underscore a critical trade-off in antenna design: high performance often comes at the cost of scalability and affordability. To balance these concerns, the present work adopts a hybrid approach using biodegradable PLA and low-cost copper thin films. This method supports environmentally responsible fabrication while maintaining competitive performance.

Building on this foundation, the antenna geometry is enhanced using a star-shaped patch, which offers advantages such as multiband behavior, longer effective current paths, and increased edge radiation. These characteristics contribute to bandwidth and improve gain without enlarging the antenna footprint [6, 13]. In this work, we present the development of a novel star-shaped microstrip patch antenna fabricated on a biodegradable PLA substrate with copper thin films. The antenna incorporates a half-elliptical ground plane to broaden the bandwidth and enhance gain performance.

The proposed antenna targets the ISM band around 2.45 GHz, suitable for applications like WLAN, Bluetooth, and IoT.

Simulation and experimental results demonstrate the effectiveness of the design, offering a low-cost, eco-friendly alternative to traditional FR4-based antennas.

2. Design Assumptions and Materials

2.1. Design Assumptions

The star-shaped patch antenna is designed for operation within the 2.45 GHz ISM band. Key performance goals include low return loss, wide impedance bandwidth, and moderate gain suitable for short-range communication systems. The –10 dB return loss threshold, equivalent to a Voltage Standing Wave Ratio (SWR) of approximately 1.93, is commonly used in antenna engineering to define acceptable impedance matching [1-2]. In this study, an SWR level of 2:1 with –10 dB return loss threshold was adopted as the upper boundary for the operating bandwidth, ensuring that the antenna maintains efficient power transfer throughout its working range. A sustainable design approach was adopted, using PLA as the dielectric substrate and copper thin film for conductivity. Design targets were verified through software simulations and later validated via measurements.

2.2. Material Properties

The antenna prototype was fabricated using a 3D-printed PLA substrate and copper thin films. The key material properties are summarized in Table 1.

Table 1. Material property parameters

Material	Property	Value	Reference/Notes
PLA	Relative Permittivity (ε_R)	2.4	Based on [9], typical for commercial 3D-printed PLA at 2–3 GHz
	Loss Tangent	0.02	Estimated from available data [9,10]
Copper Thin Film	Conductivity (σ)	5.8×10^7 S/m	Standard value for pure copper
	Thickness	35 µm	As specified for copper tape in [14]

The dielectric constant of PLA was assumed to be 2.4, based on prior research [9]. Accurate determination of substrate permittivity, particularly in the UHF band, is crucial for reliable antenna design, as small variations can significantly affect the resonance frequency and impedance bandwidth [15]. The use of PLA, a biodegradable material derived from renewable resources, aligns with sustainable manufacturing practices. Additionally, the copper thin film offers excellent electrical conductivity while enabling simple fabrication without the need for chemical etching processes, thereby minimizing environmental impact.

3. Antenna Design and Optimization

3.1. Triangular Patch Antenna on FR4 Substrate

An initial triangular patch antenna was designed on an FR4 substrate, selected for its low cost, ease of availability, and consistent dielectric properties 4.5, a commonly accepted value for FR4 as cited in [1, 16], and loss tangent equal to 0.02. The FR4 thickness was set at 1.6 mm, a common value for printed circuit board applications that supports mechanical stability while accommodating typical microstrip feed line widths for 50-ohm matching.

The dimensions of the triangular patch were calculated based on the standard transmission line model for microstrip antennas [17,18], targeting a resonant frequency of 2.45 GHz. The side of the equilateral triangular patch was determined using the following relations:

(1) $$W_p = \frac{2c}{3 f_r \sqrt{\varepsilon_r}}$$

(2) $$L_p = \sqrt{W_p^{\,2} - \left(\frac{1}{2}\times W_p\right)^2}$$

where
- c Speed of light in free space
- f_r Desired resonant frequency
- ε_r Relative permittivity of substrate
- W_p The width of the triangular patch antenna
- L_p The length of the triangular patch antenna

The ground plane width (W) and length (L) are also determined by:

(3) $$W = 6h_S + W_p$$

(4) $$L = 6h_S + L_p$$

where h_S The substrate thickness

The calculated and optimized dimensions were used to create the antenna model, which was simulated using CST Studio Suite 2023 [19]. The structure was fed with a microstrip line optimized for impedance matching at 50 Ω.

Simulation results for the FR4-based triangular patch antenna, shown in Fig. 1, indicated a central resonant frequency of 2.458 GHz, with a return loss (S_{11}) of -20.03 dB, as illustrated in Fig. 2.

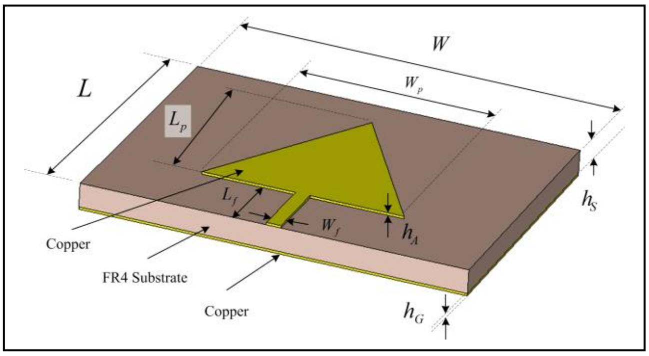

Fig. 1. Triangular patch antenna model (FR4)

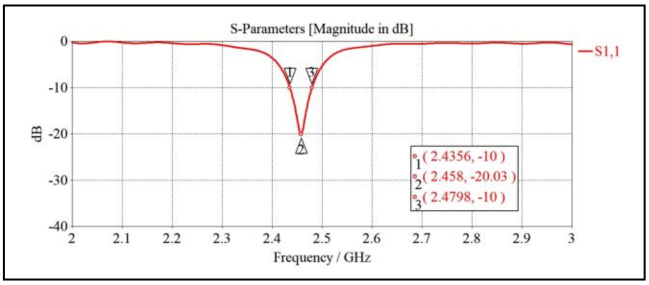

Fig. 2. S_{11} of the optimal triangular patch antenna with FR4 materials

3.2. Star-Shaped Patch with Inset-Feed

To further enhance the antenna's bandwidth and radiation characteristics, the triangular patch was modified into a star-shaped configuration by incorporating an inverted triangle at its center.

This geometric modification increases the effective current path length, thereby enhancing the bandwidth performance. Additionally, the feeding method was changed to an inset feed, which improves impedance matching without the need for external matching circuits [2]. The proposed star-shaped patch antenna design, implemented on an FR4 substrate, is illustrated in Fig. 3.

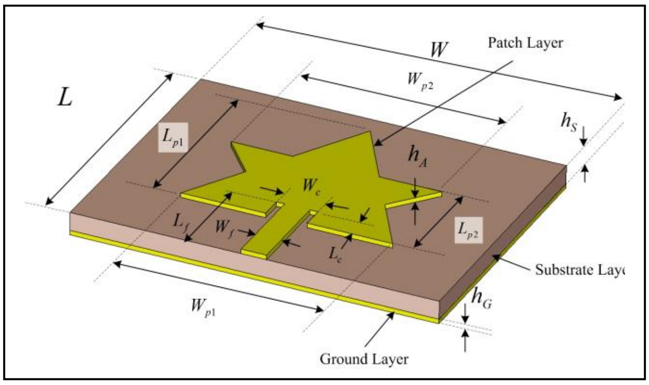

Fig. 3. Star-shaped patch antenna with FR4.

3.3. Modified Ground Plane (MGP) Technique

While the star-shaped patch improved the bandwidth, additional optimization was performed by modifying the ground plane, as previous studies have demonstrated that appropriate ground plane modifications can significantly enhance both gain and bandwidth [13].

The ground plane was modified from full size (L) to a partial rectangular ground (L_g) to suppress surface waves and enhance bandwidth as shown in Fig.4. The ground plane length was systematically varied to determine the configuration that provided the widest bandwidth and optimal impedance matching. In most designs, the ground plane length closely approximates that of the microstrip feed [20]. Subsequently, the rectangle MGP was modified to a half-elliptic shape (Fig. 5). The optimization was carried out through parametric sweeps using CST, with the final geometry selected based on a trade-off between return loss and radiation efficiency. The optimized geometric parameters of the final antenna design are summarized in Table 2.

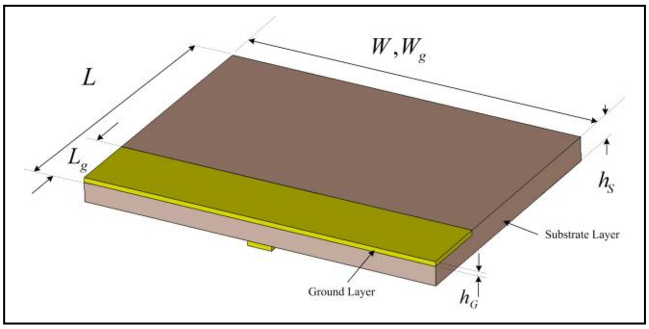

Fig. 4. Star-shaped patch antenna with rectangle MGP.

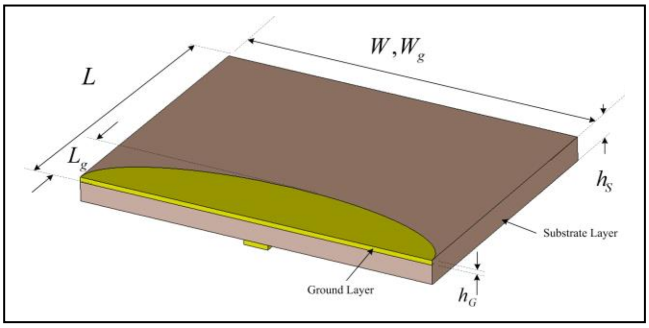

Fig. 5. Star-shaped patch antenna with half-elliptical MGP.

Table 2. Design parameters of the star-shaped patch antenna with modified ground plane using FR4

Name of Parameter	Value (mm)	Name of Parameter	Value (mm)
W	80.00	L	60.00
W_{p1}	43.00	L_{p1}	33.00
W_{p2}	35.00	L_{p2}	28.00
W_c	9.00	L_c	3.00
W_f	4.50	L_f	15.00
W_g	80.00	L_g	15.00
h_A, h_G	0.035	h_S	1.60

Simulation results, presented in Fig. 6, show that the final optimized star-shaped patch antenna with the MGP based on FR4 achieved a wide impedance bandwidth ranging from 2.0337 GHz to 3.0212 GHz, with a resonant return loss (S_{11}) of -34.011 dB at 2.4169 GHz.

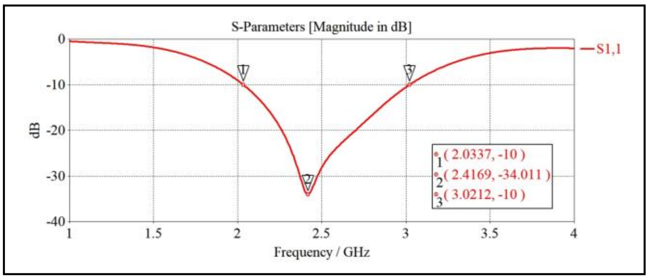

Fig. 6. S_{11} of the star-shaped patch antenna with modified ground plane using FR4.

3.4. Star Patch Antenna on PLA Substrate and Copper Thin Films

To pursue an environmentally friendly design, the FR4 substrate was replaced with 3D-printed PLA. Due to the lower dielectric constant of PLA, the patch dimensions were re-optimized to maintain resonance at approximately 2.45 GHz.

In this design, the conductive layers on both the top and bottom surfaces are formed using thin copper films. The thickness of the top conductive layer, denoted as h_A, and the thickness of the bottom conductive layer, denoted as h_G. Typically, copper film thicknesses for such applications range between 17 µm (1/2 oz/ft²) and 35 µm (1 oz/ft²). For this study, a thickness of approximately 35 µm was adopted for both h_A and h_G, ensuring adequate current-carrying capability, minimizing conductor losses at the operating frequency of 2.45 GHz, and maintaining mechanical robustness during the handling and post-processing stages.

The dielectric substrate itself, fabricated using biodegradable polylactic acid (PLA), possesses a thickness denoted as h_S. For consistency with traditional PCB-based designs and to facilitate comparative analysis, the substrate thickness was aligned with that commonly found in commercial FR4 boards. Standard FR4 substrates used in microwave and RF designs often have thicknesses in the range of 0.2 mm to 3.2 mm [16]. Accordingly, an h_S of approximately 1.6 mm was selected for this work.

Table 3 presents the optimized dimensions for the star-shaped patch antenna. These dimensions were determined based on achieving a 10 dB return loss and satisfactory radiation efficiency. The antenna features a modified ground plane and is fabricated using PLA and a copper thin film. Simulation results (Fig. 7) show that the optimized antenna achieved an impedance bandwidth from 2.0007 GHz to 3.0823 GHz, with a resonant return loss (S_{11}) of -30.213 dB at 2.456 GHz. Furthermore, the radiation patterns were evaluated, confirming quasi-omnidirectional coverage in the horizontal plane (Figs. 8 and 9) and a broadside (Z-axis) gain of approximately 2.32 dB.

Table 3. Design parameters of the proposed antenna

Name of Parameter	Value (mm)	Name of Parameter	Value (mm)
W	80.00	L	60.00
W_{p1}	35.30	L_{p1}	35.00
W_{p2}	30.00	L_{p2}	28.00
W_c	7.00	L_c	8.00
W_f	3.00	L_f	15.00
W_g	80.00	L_g	15.00
h_A, h_G	0.035	h_S	1.60

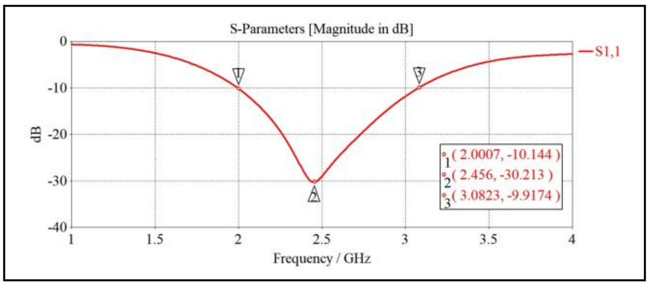

Fig. 7. S_{11} of the star-shaped patch antenna with modified ground plane using PLA and copper thin film materials.

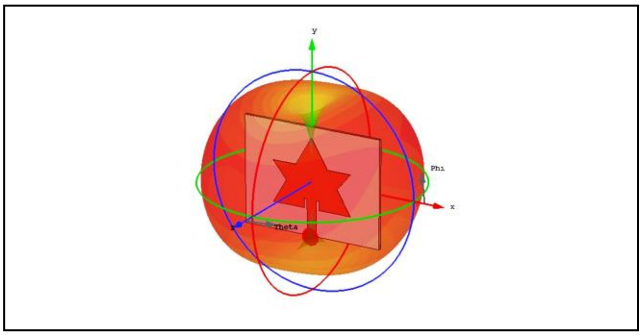
Fig. 8. 3D radiation pattern of the star-shaped patch antenna.

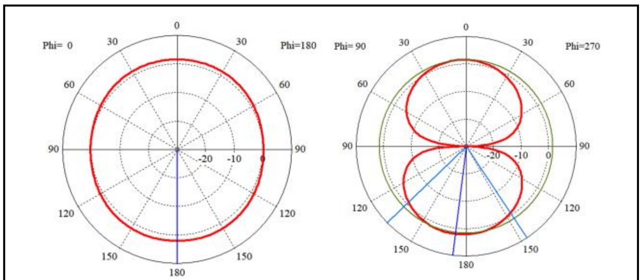

a) Horizontal plane b) Vertical plane

Fig. 9. 2D radiation pattern of the star-shaped patch antenna

4. Fabrication Process and Measurement Setup

4.1. Antenna Fabrication

The proposed star-shaped patch antenna was fabricated with a three-layer configuration: a top copper thin film for the radiating patch, a middle 3D-printed polylactic acid (PLA) substrate, and a bottom half-elliptical copper ground plane. The PLA substrate was produced using a FlashForge Creator 3 Pro 3D printer, employing standard PLA filament with 100% infill to ensure consistent and homogeneous dielectric behavior across the entire volume [21]. The copper thin films were shaped using a Silhouette Cameo 3 cutting machine [22].

The copper films were manually applied to the PLA substrate using built-in transparent acrylic adhesive sheets to ensure strong mechanical and electrical contact while minimizing additional parasitic effects. The individual antenna components, including the patch, substrate, and ground plane, are shown in Figs. 10(a–c). The fully assembled prototype is presented in Fig. 11.

4.2. Measurement Setup

The prototype antenna was measured to evaluate both impedance matching and radiation performance. The measurement setup consisted of the following elements. Impedance measurements were conducted using an Agilent E5071C Vector Network Analyzer (VNA). To minimize electromagnetic reflections and external interference during the radiation pattern measurements, a small anechoic chamber was constructed within a laboratory room. The chamber was specifically designed to accommodate compact antenna testing and was lined with LEYBOLD Microwave Absorbers (Model 737390), which are optimized for efficient absorption in the microwave frequency range [23]. The absorbers were positioned to enclose the Device Under Test (DUT) antenna on all sides, including the floor and walls within the immediate vicinity of the antenna. This setup suppressed multipath reflections and reduced measurement uncertainty. It ensured a controlled, reflection-free environment for reliable gain and pattern measurement. Its installation within a conventional laboratory space demonstrated a cost-effective and practical solution for accurate antenna characterization in space-constrained settings.

For gain comparison, two identical prototype antennas were evaluated using the two-antenna method, following the standard procedure described in [2]. The antenna under test was rotated using a DreamCatcher ME1300 antenna lab test system, enabling automated angular measurements [24].

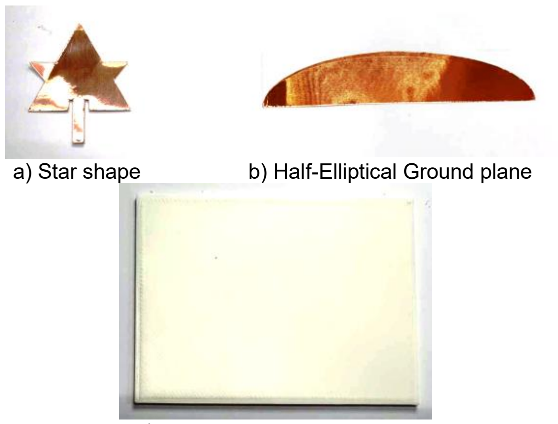
a) Star shape b) Half-Elliptical Ground plane

c) Rectangular PLA substrate

Fig. 10. Fabrication of patch, ground, and PLA substrate.

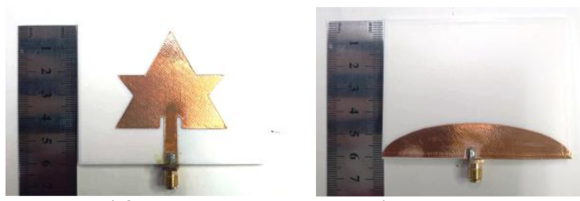
a) front view b) back view

Fig. 11. Prototype of the proposed antenna.

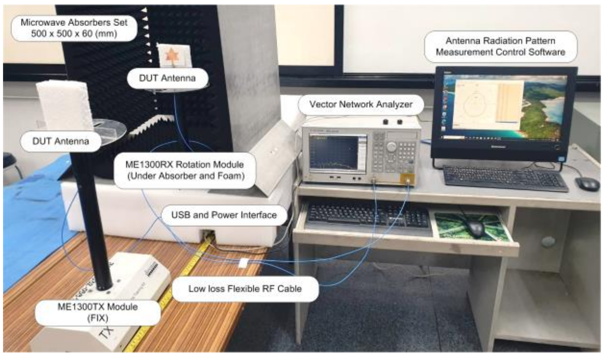

Fig. 12. Radiation pattern measurement setup.

Figure 12 shows the measurement setup used to obtain the radiation patterns and gain. The test environment was designed to minimize reflections and external interference, ensuring the reliability of the measurement results.

4.3. Measurement Results

The return loss ($|S_{11}|$) of the fabricated antenna was measured and compared against simulation results (Fig. 13).

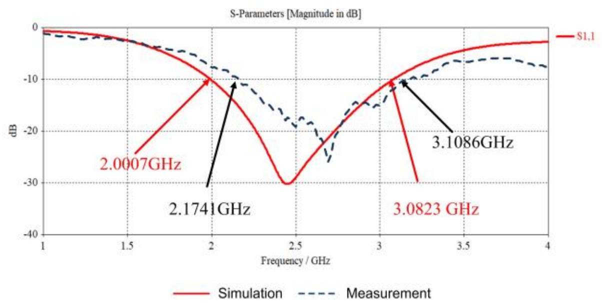

Fig. 13. Comparison of S_{11} between simulation and measurement

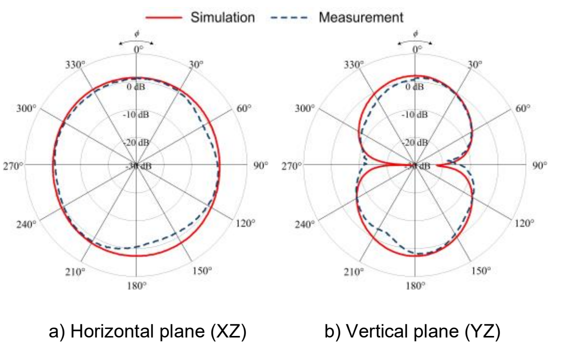

Fig. 14. Comparison of 2D radiation patterns from simulation and measurement.

The measured bandwidth for $S_{11} < -10$ dB ranged from 2.1741 GHz to 3.1086 GHz, closely matching the simulated range of 2.0007 GHz to 3.0823 GHz.

The 2D radiation patterns measured in the XZ and YZ planes are shown in Fig. 14. The horizontal plane pattern approximates an omnidirectional radiation characteristic, while the vertical plane shows a bi-directional pattern consistent with simulation results. The measured peak gain was 2.13 dB, compared to the simulated value of 2.32 dB, representing an acceptable deviation of approximately 8.54%.

5. Results and Discussion

The simulation results, presented in Fig. 6 and Fig. 7, show that the optimized FR4-based antenna achieved a wide impedance bandwidth ranging from 2.0337 GHz to 3.0212 GHz, with a resonant return loss (S_{11}) of –34.011 dB at 2.4169 GHz. Although this bandwidth is slightly narrower than that of the PLA-based antenna (2.0007–3.0823 GHz), it still meets wideband performance criteria.

The measured and simulated reflection coefficients ($|S_{11}|$) of the proposed star-shaped patch antenna, shown in Fig. 13, exhibit good agreement. The simulated antenna achieved a –10 dB impedance bandwidth from 2.0007 GHz to 3.0823 GHz, while the measured prototype demonstrated a slightly broader range from 2.1741 GHz to 3.1086 GHz. The center frequencies were closely aligned, with minor deviations primarily attributed to variations in the dielectric constant and loss tangent of the 3D-printed PLA material, small mechanical tolerances during cutting and assembly, and the influence of the SMA connector and measurement cables.

Figure 14 illustrates the 2D radiation patterns of the proposed antenna in both the XZ-plane (horizontal) and YZ-plane (vertical), comparing simulated and measured results. In the horizontal plane, the radiation pattern is nearly omnidirectional, which is advantageous for various wireless communication applications. In the vertical plane, a bi-directional pattern is observed, with slight asymmetry in the measured results, primarily attributed to the physical test setup. The measured gain was 2.13 dB, closely aligning with the simulated gain of 2.32 dB, which is considered acceptable given the use of additive manufacturing and manual assembly techniques in the prototyping process.

The incorporation of a half-elliptical modified ground plane (MGP) significantly enhanced the antenna's bandwidth by altering the surface current distribution. This final MGP design represents an optimized trade-off between bandwidth improvement and reliable radiation performance. While other ground plane shapes were explored, the half-elliptical structure provided the best balance of bandwidth, gain, and fabrication simplicity.

Table 4. Comparison of the designed antenna with existing antennas

Ref.	Process	Material	Recycle material	Frequency (GHz)	Bandwidth (GHz)	Gain (dB)
[6]	Etching	FR4	No	3.00	1.98–4.30	2.10
[9]	Full 3D Printing	Electrifi + PLA	Yes	2.45	2.04–2.59	2.35
[25]	Etching	FR4	No	2.4 /5.0	2.30-2.50 /5.00-5.30	1.9 /2.36
[26]	Etching	RT-Duroid	No	2.48	2.40–2.48	8.00
[27]	Textile Lamination	Textile + Conductive Fabric	Partially	2.45	2.42–2.48	2.20
This Work	3D Printing + Cutting	PLA + Copper Thin Film	Yes	2.45	2.17–3.10	2.13

Finally, table 4 summarizes the key performance metrics of the proposed antenna in comparison with related works operating in similar frequency bands and utilizing comparable materials. The proposed design, which employs a sustainable fabrication approach combining 3D printing and cutting using PLA and copper thin film, demonstrates a favorable balance between performance and environmental sustainability. Operating at 2.45 GHz, it achieves a wide impedance bandwidth of 2.17–3.10 GHz and a measured gain of 2.13 dB.

While its gain is moderate compared to high-performance designs such as [26], which reports 8.00 dB using RT-Duroid, the proposed antenna offers broader bandwidth than most other works, including the dual-band antenna in [25]. Moreover, the incorporation of recycled materials and cost-effective fabrication techniques distinguishes this work as an environmentally friendly and practical alternative to conventional methods.

6. Conclusions

This study introduced a star-shaped patch antenna with a half-elliptical modified ground plane, fabricated using a 3D-printed PLA substrate and copper thin films. Aimed at creating a cost-effective, eco-friendly alternative to FR4-based antennas, the design maintained strong performance for 2.45 GHz ISM-band applications. Key features include enhanced bandwidth via the star-shaped patch and improved impedance matching through the modified ground plane.

The PLA-based antenna achieved broader bandwidth than its FR4 counterpart, with simulations and measurements closely aligned. It exhibited a simulated bandwidth of 2.0007–3.0823 GHz and a gain of 2.32 dB, while measurements showed 2.1741–3.1086 GHz with a 2.13 dB gain. The PLA version's resonant frequency was 1.6% higher.

In summary, the PLA antenna offers slightly better bandwidth, comparable performance, and notable advantages in sustainability and ease of fabrication, validating its suitability for IoT and wireless applications.

This research project is supported by Rajamangala University of Technology Isan. Contract No. ENG8/67. The authors express their sincere gratitude to the reviewers for their valuable comments and suggestions, which significantly improved the quality and clarity of this manuscript. Special thanks are also extended to Mr. Chanurak Chinnampong for his assistance in the preparation and measurement of the prototype antenna.

Authors: *Charinsak Saetiaw, Department of Electronics and Telecommunication Engineering. Faculty of Engineering, Rajamangala University of Technology Isan, Khon-Kean Campus, Thailand. E-mail: charinsak.sa@rmuti.ac.th; Jatuporn Nakorntep, Studying in Electrical Engineering (master's degree), Department of Electronics and Telecommunication Engineering. Faculty of Engineering, Rajamangala University of Technology Isan, Khon-Kean Campus, Thailand E-mail: jatuporn.na@rmuti.ac.th*; *Vithaya Chamnanphrai, Department of Electronics and Telecommunication Engineering, Faculty of Engineering, Rajamangala University of Technology Isan Khonkaen Campus, Thailand, E-mail: vithaya.ch@rmuti.ac.th; Suthasinee Lamultree, Department of Electronics and Telecommunication Engineering, Faculty of Engineering, Rajamangala University of Technology Isan Khonkaen Campus, Thailand, E-mail: suthasinee.la@rmuti.ac.th.*

REFERENCES

[1] Balanis C.A., *Antenna Theory: Analysis and Design*, 4th ed., Wiley, 2016.
[2] Milligan T.A., *Modern Antenna Design*, 2nd ed., John Wiley & Sons, 2005.
[3] Khan M.U., Sharawi M.S., Mittra R., Microstrip patch antenna miniaturization techniques: A review, *IET Microwaves Antennas Propagation*, 9 (2015), No. 9, 913–922.
[4] Lamultree S., Jansri C., Phongcharoenpanich C., Design of a compact wideband circular monopole antenna for 5G applications, *Przegląd Elektrotechniczny*, 97 (2021), No. 4, 9–21.
[5] Mondal K., Sarkar P.P., Enhancement of the gain and bandwidth of the microstrip patch antenna with modified ground plane, *Int. J. Microwave Wireless Technol.*, 9 (2017), No. 5, 1179–1184.
[6] Pandey M.S., Chaudhary V.S., Defected star-shaped microstrip patch antenna for broadband applications, *Progress In Electromagnetics Research C*, 118 (2022), 11–24.
[7] Bithell T., New report explores recyclable materials for PCBs, *Envirotec*, 22 April 2025. [Online]. Available: https://envirotecmagazine.com/2025/04/22/new-report-explores-recyclable-materials-for-pcbs/
[8] Jankowski-Mihułowicz P., Węglarski M., Wilczkiewicz B., Chamera M., Laskowski G., The influence of textile substrates on the performance of textronic RFID transponders, *Materials*, 15 (2022), No. 20, 7060.
[9] Saetiaw C., Phuchaduek S., 3D printed capsule-shaped dipole with multi-slot antenna based on metallic filament material, *Przegląd Elektrotechniczny*, 97 (2021), No. 8, 48–51.
[10] Aziz M., El Hassan A., Hussein M., Zaneldin E., Al-Marzouqi A.H., Ahmed W., Characteristics of antenna fabricated using additive manufacturing technology and the potential applications, *Heliyon*, 10 (2024), No. 6, Art. e27785.
[11] Moallem M.H., Shamim A., Tentzeris M.M., Parametric study of 3D additive printing parameters using conductive filaments on microwave topologies, in: *Proc. IEEE MTT-S Int. Microwave Symp. (IMS)*, (2019), 1127–1130.
[12] Helena D., Ramos A., Varum T., Mato J.N., The use of 3D printing technology for manufacturing metal antennas in the 5G/IoT context, *Sensors*, 20 (2020), No. 21, 5997.
[13] Mondal K., Sarkar P.P., Enhancement of the gain and bandwidth of the microstrip patch antenna with modified ground plane, *Int. J. Microwave Wireless Technol.*, 9 (2017), No. 5, 1179–1184.
[14] 3M™, Copper Foil Tape 1126, 3M Company. [Online]. Available: 3M Official Website.
[15] Jankowski-Mihułowicz P., Lichoń W., Pitera G., Węglarski M., Determination of the material relative permittivity in the UHF band by using T and modified ring resonators, *Int. J. Electron. Telecommun.*, 62 (2016), No. 2, 129–134.
[16] Nascimento D.C., da S. Lacava J.C., Design of low-cost probe-fed microstrip antennas, *InTechOpen*, 2011. [Online]. Available: https://www.intechopen.com/chapters/20818
[17] Zhang S., A review of planar antennas for millimeter wave 5G network, *Highlights Sci. Eng. Technol.*, 27 (2022), 662–670.
[18] Vishwakarma R.K., Ansari J.A., Meshram M.K., Equilateral triangular microstrip antenna for circular polarization dual-band operation, *Indian J. Radio Space Phys.*, 35 (2006), No. 4, 293–296.
[19] *CST Studio Suite®*, Academic Version, Dassault Systems, 2023.
[20] Zulkifli F.Y., Wahdiyat A.I., Zufar A., Nurhayati N., Setijadi E., Super-wideband monopole printed antenna with half-elliptical-shaped patch, Telecom, 5 (2024), No. 3, 760–773,
[21] Moscato S., Bahr R., Le T., Pasian M., Bozzi M., Perregrini L., Tentzeris M., Infill-dependent 3D-printed material based on NinjaFlex filament for antenna applications, *IEEE Antennas Wireless Propag. Lett.*, 15 (2016), 1506–1509.
[22] Silhouette America, Inc., *Silhouette Cameo 3 Electronic Cutting Machine*. [Online] Available: https://www.silhouetteamerica.com
[23] LEYBOLD Didactic GmbH, *Microwave Absorber, Model 737390*, Huerth, Germany. [Online]. Available: https://www.ld-didactic.com/
[24] DreamCatcher Asia, *ME1300 Antenna and Propagation Courseware*, [Online]. Available: https://www.dreamcatcher.asia
[25] Lamultree S., Somsanook N., Narkkoht W., Phongcharoenpanich C., A dual-band rectangular shape incorporated into circular patch antenna for 2.4/5 GHz wireless local area network applications, *TELKOMNIKA (Telecommunication Computing Electronics and Control)*, 23 (2025), No. 1, 1–8. 10.12928/telkomnika.v23i1.26519.
[26] John M., Manoj B., Chandran J.G., Design of slotted rectangular microstrip patch antenna operated in ISM band using RT-Duroid substrate, in: *Proc. Natl. Conf. Signal Processing, Instrumentation and Communication Engineering (SPICE'16)*, 2016.
[27] Saetiaw C., Phuchaduek S., The design and measurement of modified capsules-shaped patch antenna with textile material, *Engineering Access*, 7 (2021), No. 2, 126–130.